Tunable Super-Structured Fiber Bragg Gratings with Perfect Sequences Based on *m*-Sequence

João S. Pereira, Marco P. M. Ferreira, and Marko Gasparovic

***Abstract*—Recently, a tunable fiber Bragg grating (FBG) was developed by using stress-responsive colloidal crystals. In this paper, we have simulated the application of these nanoparticles into the super-structured fiber Bragg grating (SSFBG) written with perfect sequences derived from a short maximal-length sequence. A tunable SSFBG will be available to overcome the prohibitive temperature variation of the optical codecs. Nevertheless, we presented a method to implement coherent time spreading optical code-division multiple-access (OCDMA) where a unique code (or perfect sequence) can be reused and mixed with different wavelengths to obtain a tunable wavelength-division multiplexing (WDM) system. In order to maximize the binary throughput, we have selected a unique short maximal-length sequence composed of 7 chips that can be tuned with 7 different optical wavelengths. We found thousands of different tunable combinations that presented power contrast ratios (*P*/*C*) higher than 12 dB. When a WDM-OCDMA system used 2 different combinations simultaneously, the perfect binary detection with error correction codes was achieved successfully. The tunable SSFBG with colloidal crystals will be a simple and good alternative choice for fiber-to-the-home (FTTH) communications.**

***Index Terms*—Optical code-division multiple-access (OCDMA), super-structured fiber Bragg grating (SSFBG), wavelength-division multiplexing OCDMA (WDM-OCDMA).**

1. Introduction

Optical fibers provide an enormous and unsurpassed transmission bandwidth with negligible latencies, and are now one of the transmission media for the long distance and high data rate transmission in telecommunication networks[1]-[4].

Manuscript received June 26, 2016; revised July 17, 2017.

J. S. Pereira (corresponding author) and M. Gaparovic are with the Instituto de Telecomunicações, Lisboa 1049-001, Portugal and also with Institute Polytechnic of Leiria, Leiria 2411-901, Portugal (e-mail: joao.pereira@ipleiria.pt; marko1559@gmail.com).

M. P. M. Ferreira is with the Centro de Investigação em Informática e Comunicações, Institute Polytechnic of Leiria, Leiria 2411-901, Portugal (e-mail: marco.ferreira@ipleiria.pt).

Color versions of one or more of the figures in this paper are available online at http://www.journal.uestc.edu.cn.

Digital Object Identifier: 10.11989/JEST.1674-862X.70912063

Optical code-division multiple access (OCDMA) is a promising candidate for next-generation broadband access networks. Super-structured fiber Bragg gratings (SSFBGs) can be used as encoders/decoders on time spreading optical code-division multiple access (TS-OCDMA) communication, offering high performance, compactness, and compatibility with fiber-optic systems with a potential low cost[5]-[13].

The optical performance with high throughput passes through the use of optical codecs and decoders that can perform this task in optical domain and in real time. It is possible to find many kinds of optical codecs. Some of them are planar light wave circuits[14], spatial light wave phase modulators[15], and arrayed waveguide gratings[16]. However, all of them require a temperature stability. For example, if the temperature range between two optical network units (ONUs) of a fiber-to-the-home (FTTH) system is larger than 8.0 K, the temperature controller for the SSFBG should be installed in each ONU[3]. To avoid this problem, in this paper we will present a new optical SSFBG codec that is tunable and can, by this way, compensate the temperature drift. Nevertheless, the tunable SSFBG can also implement a simple wavelength multiplexing process between different users.

Fiber Bragg gratings (FBGs) are optical fibers which were developed by using stress-responsive colloidal crystals that can reflect particular wavelengths of light and transmit all others[1]. The FBG is a periodic perturbation of the refractive index along the fiber length which is formed by exposure of the core to an intense optical interference pattern[17]. An SSFBG, also called a sampled FBG, is a special FBG that consists of several small FBGs placed in close proximity to one another. SSFBGs have attracted much attention in recent years with the discovery of techniques allowing the creation of equivalent chirp or equivalent phase shifts. The biggest advantage of an SSFBG with equivalent chirp or equivalent phase shifts is the possibility to design and fabricate gratings with greatly varying phase and amplitude responses by adjusting the spatial profile of the superstructure[18]. The SSFBG technology has been shown to provide an attractive and highly flexible route to produce high-performance and potentially low-cost code generation and recognition components as required for direct sequence (DS) OCDMA systems[19]. In this paper, we present the integration of SSFBG with a tunable mechanism where the thickness of the nanomaterial can be adjusted to reduce the error probability in an optical communication system. A based

piezoelectric device can control this thickness with precision. Also, these FBGs are using stress-responsive colloidal crystals as their Bragg reflectors which have interesting optical properties, such as photonic band gaps (PBGs)[1]. This feature is responsible for making colloidal crystals optimal candidates for the construction of FBGs with a tunable filter or reflector, depending on the objective. It can also have the function of filtering multiple wavelengths by incorporating different colloidal crystal segments into the fiber[1]. The problem is that if we have fixed the colloidal crystal film, then the tuning ranges of the PBGs are mostly limited by their refractive index parameters. There is a necessity to alter the distance between neighboring colloidal crystals films to reduce the refractive index.

The main peak position (for a chip i) can be estimated by Bragg's equation[1] for a normal incident beam:

$$\lambda_i = 1.633 d_i n_{\text{average}} \tag{1}$$

where d_i is the distance between two adjacent nanoparticles and n_{average} is the average refractive index of the colloidal crystal films i. By definition, in digital communications a chip is a pulse of a pseudo-random noise (PN) code sequence used in DS code division multiple access (CDMA) techniques.

Based on (1), there are several protocols for tuning the PBGs of the films which are placed on the proximal end faces of two sections of optical fibers. A good example of tuning the PBG is changing the distance between neighboring colloidal crystals with mechanical stress. Its PBG can be tuned precisely by using different strengths of pressure.

Tunable FBGs, using responsive colloidal crystals, have characteristic reflection peaks of the FBG shifts when compression is applied to them. Furthermore, it has been found that the shift is linearly dependent with the compression ratio[1]. Let the compression ratio of the reflector R_i be defined as

$$R_i = 1 - (T_i / T_0) \tag{2}$$

with T_i being the compressed thickness of the colloidal crystal Bragg reflector and T_0 being its initial thickness. Then, the shifted center wavelength (λ_i) resulting from the compression can be approximated, with a 0.9899 correlation coefficient, as

$$\lambda_i = 603.1 - 385.3 R_i. \tag{3}$$

According to (3), the FBG with different Bragg reflectors could be customized precisely by quickly tuning the thicknesses of its Bragg reflectors.

In Section 2, we introduce a theoretical model for the tunable SSFBG. Section 3 presents a coherent wavelength-division multiplexing OCDMA (WDM-OCDMA) system with tunable SSFBG. The following Section 4 shows that it is possible to estimate the error probability of the tunable SSFBG, and main conclusions are gathered in the last section.

2. Theoretical Model for Tunable SSFBG

The SSFBG power reflection of the FBG i, with length L_i, is given by the following equation[17]:

$$r_i = \left| \frac{-\kappa \sinh\left(\sqrt{\kappa^2 - \hat{\sigma}^2} L_i\right)}{\hat{\sigma} \sinh\left(\sqrt{\kappa^2 - \hat{\sigma}^2} L_i\right) + \mathrm{j} \sqrt{\kappa^2 - \hat{\sigma}^2} \cosh\left(\sqrt{\kappa^2 - \hat{\sigma}^2} L_i\right)} \right|^2 \tag{4}$$

where j is the imaginary number, $\hat{\sigma} = (\lambda_{\max}/\lambda - 1)\pi N_G / L_i$, and $i = 0, 1, \cdots, N-1$. Here, $\lambda_{\max}$ is the wavelength of maximum reflectivity, that occurs when $\hat{\sigma} = 0$ and is given by $\lambda_{\max} = \left(1 + \overline{\delta n_{\text{eff}}}/n_{\text{eff}}\right)\lambda_i$. To simplify the study of SSFBG, it is possible to consider that $\lambda_{\max} \approx \lambda_i$. Here λ_i is the design wavelength of the FBG i for Bragg scattering by an infinitesimally weak grating[17]. n_{eff} is the refractive index. For a single-mode Bragg reflection with a uniform grating, the "dc" index change[17] spatially averaged over a grating period $\overline{\delta n_{\text{eff}}}$ is constant. Therefore, the coefficients $\hat{\sigma}$ and κ are also constants. κ is the "ac" coupling coefficient and $\hat{\sigma}$ is a general "dc" self-coupling coefficient used in the coupled-mode theory of uniform gratings, where N_G is the total number of grating periods[17].

The usage of responsive colloidal crystals in a SSFBG is represented in Fig. 1 with the R_i blocks, where Δz_i is the value of the separation between two chips. The N sections of length L_i have a tunable thickness T_i of colloidal crystals with a compression R_i. The N sections of length L_i are written by using the wavelength $\lambda_i = \lambda_0 + i\Delta\lambda$, where $\Delta\lambda$ is an incremental value of the wavelength ($\Delta\lambda << \lambda_0$). Each section of the grid represents a SSFBG chip that is etched with a phase ϕ_i, $i = 0, 1, \cdots, N-1$.

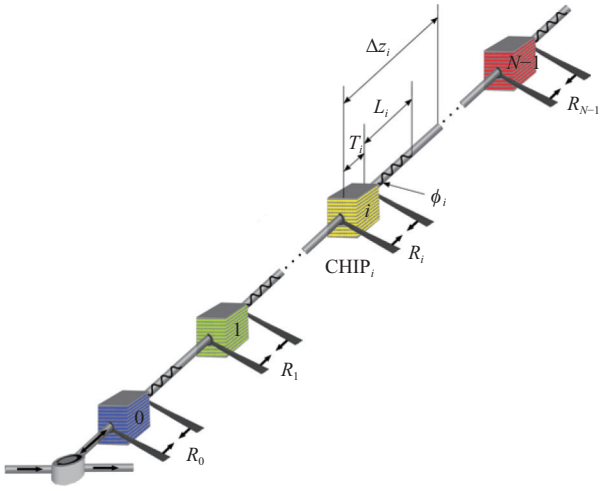

Fig. 1. Tunable SSFBG encoder structure.

For our SSFBG study (based on a selected family of codes) we considered that $\Delta z_i \geq \max(T_i + L_i)$. The power reflection (4) can be rewritten using a Taylor series for sinh(·) and cosh(·) when $\sqrt{\kappa^2 - \hat{\sigma}^2} L_i$, $i = 0, 1, \cdots, N-1$, assumes a low value.

Thus, the power reflection of a chip i has been derived and it is approximately[2]:

$$r_i(\lambda) \approx \left| \frac{-\kappa_1 L_i}{\pi N_G / L_i (\lambda_{\max}/\lambda - 1) + \mathrm{j}} \right|^2. \quad (5)$$

This expression is similar to the transfer function of a bandpass filter (BPF) centered on the wavelength $\lambda_{\max}$, with the amplitude $r_i(\lambda_{\max}) = |\kappa_1 L_i|^2$ and

$$r_i(\pm\infty) = \frac{|\kappa_1 L_i|^2}{1 + (\pi N_G / L_i)^2} = \varepsilon |\kappa_1 L_i|^2. \quad (6)$$

When $\pi N_G >> L_i$, then $r_i(\lambda_{\max}) >> r_i(\pm\infty)$ (because $\varepsilon << 1$), and therefore it is possible to associate a specific SSFBG i to a BPF.

In this scenario, it is considered that the N chips are written with the wavelength $\lambda_i = \lambda_0 + i\Delta\lambda$, for $0 \le i \le N-1$, and all chips will have the same value $\kappa = \kappa_1$. κ_1 is a constant and equals to the "ac" coupling coefficient of all colloidal crystals. For convenience, the transfer function of the 1st chip of the SSFBG, when $\phi_0 = 0$, may be modelled as a scaled version of the rectangular function defined by the following expression:

$$\mathrm{Rect}_{\varepsilon}\left(\frac{\lambda - \lambda_{\max}}{B}\right) = \begin{cases} 1 & \text{when} \quad \lambda_{\max} - \dfrac{B}{2} \le \lambda \le \lambda_{\max} + \dfrac{B}{2} \\ \varepsilon & \text{other} \quad \lambda \end{cases}. \quad (7)$$

This special rectangular function, centered at $\lambda_{\max}$, has a bandwidth equal to B and a minimum amplitude equal to $\varepsilon = 1/\left(1 + (\pi N_G / L_i)^2\right)$. When $\pi N_G >> L_i$, then $B \approx 2L_i\lambda_{\max}/\pi N_G$, and (7) is cut –3 dB at $\lambda = \lambda_{\max} \pm B/2$. Each grid of each SSFBG chip i, $i = 0, 1, \cdots, N-1$, acts as a specific BPF with a transfer function approximately equal to the following expression:

$$|\kappa_1 L_i|^2 \exp\{\mathrm{j}\phi_i\} \mathrm{Rect}_{\varepsilon}\left(\frac{\lambda - \lambda_0 - i\Delta\lambda}{B}\right). \quad (8)$$

It was considered that $\lambda_{\max} \approx \lambda_i$. The phase ϕ_i of the chip i is shown in Fig. 1. The power reflection of a series of N chips (a train of N FBGs) is given by

$$\prod_{i=1}^{N} |\kappa_1 L_i|^2 \exp\{\mathrm{j}\phi_i\} \mathrm{Rect}_{\varepsilon}\left(\frac{\lambda - \lambda_0 - i\Delta\lambda}{B}\right). \quad (9)$$

Considering the special case when $B/2 \le \Delta\lambda < B$, then the previous expression may be considered approximately equal to

$$\sum_{i=0}^{N-1} A^2 \exp\{\mathrm{j}(\phi_i + \phi_{i+1})\} \mathrm{Rect}_{\varepsilon_2}\left(\frac{\lambda - \lambda_0 - i\Delta\lambda - \Delta\lambda/2}{W}\right) \quad (10)$$

with $A^2 = \varepsilon^{N-2} |\kappa_1 L_i|^4$ and $\varepsilon_2 = \varepsilon / |\kappa_1 L_i|^2$.

This result of (10) is obtained when the product of two consecutive rectangular functions (of index i and index i+1) is equal to a rectangular function with a bandwidth $W = B - \Delta\lambda$, with $0 < W < B$, centered at $\lambda_0 + i\Delta\lambda + \Delta\lambda/2$. In this process, $\varepsilon_2 = \varepsilon / |\kappa_1 L_i|^2$ can be disregarded if (10) is sampled at the centers of rectangular pulses $\mathrm{Rect}_{\varepsilon_2}((\lambda - \lambda_0 - i\Delta\lambda - \Delta\lambda/2)/W)$. The sampling process is equivalent to considering that the bandwidth W is reduced to an infinitesimal value. This operation will convert (10) in a function approximately equal to a train of unit pulses. That is, the SSFBG power reflection of N chips (uniformly distributed) is approximately equal to (10) after the sampling procedure defined by

$$\sum_{i=0}^{N-1} A^2 \exp\{\mathrm{j}(\phi_i + \phi_{i+1})\} \delta\left(\lambda - \lambda_0 - i\Delta\lambda - \frac{\Delta\lambda}{2}\right). \quad (11)$$

The function $\delta(\cdot)$ is a unitary pulse. For convenience, it is considered that $\phi_N = \phi_0$. In other words, the power reflection has undergone a translation of one cycle. This simplification can be made if the codes written in SSFBGs are considered long ($N >> 2$). In this case, the inverse discrete Fourier transform (IDFT) of a normalized SSFBG power reflection (IDFT of (11) around $\lambda_0 + \Delta\lambda/2$) is approximately proportional to the following expression:

$$x_{\mathrm{SSFBG}}(t) \propto \sqrt{N}\mathrm{IDFT}\left\{\sum_{i=0}^{N-1} \exp[\mathrm{j}(\phi_i + \phi_{i+1})] \delta(\lambda - i\Delta\lambda)\right\} \quad (12)$$

when the input of the SSFBG is a unitary pulse with an amplitude $\sqrt{N}/A^2$. After the $\lambda_0 + \Delta\lambda/2$ translation of (11), this signal (12) can be considered as a baseband signal of the codes written in the SSFBG.

Each chip Δz_i of a SSFBG, when $B/2 \le \Delta\lambda < B$, has a phase $\theta_i = \phi_i + \phi_{i+1}$ defined by the cosine pattern (L_i of Fig. 1) and the stress-responsive colloidal crystals (T_i of Fig. 1). The amplitudes must be constant for all chips. This means that the SSFBG power reflection baseband signal, defined by the model (12), is the IDFT of a unimodular sequence. By definition, (12) is a perfect sequence[20]. This means that our tunable SSFBG codec will be immune of multipath interferences.

3. Coherent WDM-OCDMA System with Tunable SSFBG

Continuing the study, we simulated the usage of a coherent WDM-OCDMA system using a tunable SSFBG coded with a 7-chip m-sequence. The sequence used was [+1, +1, +1, –1, –1, +1, –1]. Because of the wavelength shifting properties of the compressed colloidal crystals, different wavelength channels can be chosen for each chip. Table 1 shows the 7 different channels that we used in our simulation, including the compression ratio R_i required to achieve the desired wavelength λ_i. Each channel has a bandwidth of B = 25 nm, $B/2 = \Delta\lambda$ = 12.5 nm.

By giving different tunings to each section of the SSFBG, different combinations of channels can be used to transmit the code. Our simulation includes three different scenarios of channel configurations for the same code, which we called SSFBG1, SSFBG2, and SSFBG3. Table 2 shows the scenarios

used. Notice that SSFBG3 uses only one channel. These multiple combination scenarios would also allow simultaneous users (each with a different WDM channel combination), or increase the throughput of the communications (sending multiple bits in parallel).

Table 1: Wavelength and compression ratio for the *m*-sequence of 7 chips

Channel i	Wavelength λ_i (nm)	Compression ratio R_i
0	512.5	0.235
1	525.0	0.203
2	537.5	0.170
3	550.0	0.138
4	562.5	0.105
5	575.0	0.073
6	587.5	0.040

Table 2: Different WDM combinations used to encode the *m*-sequence [+1, +1, +1, –1, –1, +1, –1].

Configuration name	WDM combination
SSFBG1	+Ch5, +Ch4, +Ch2, –Ch3, –Ch6, +Ch0, –Ch1
SSFBG2	+Ch1, +Ch0, +Ch6, –Ch4, –Ch5, +Ch2, –Ch3
SSFBG3	+Ch6, +Ch6, +Ch6, –Ch6, –Ch6, +Ch6, –Ch6

Figs. 2, 3, and 4 represent the power spectra of SSFBG1, SSFBG2 and SSFBG3 respectively. The *m*-sequence of 7 chips has been simulated by using 42 samples in the 100 nm that composes the entire 7-channels bandwidth, considering a SSFBG writing phase precision of $\pi/10$.

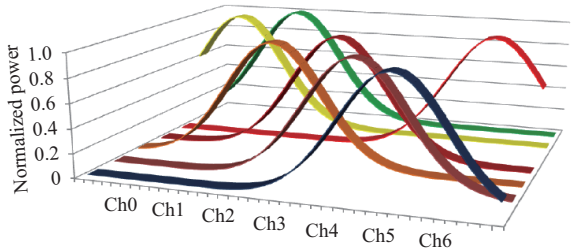

Fig. 2. Spectrum SSFBG1=+Ch5, +Ch4, +Ch2, –Ch3, –Ch6, +Ch0, –Ch1.

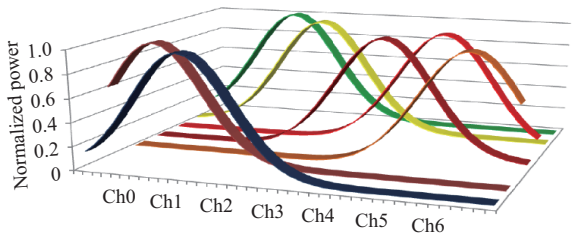

Fig. 3. Spectrum SSFBG2=+Ch1, +Ch0, +Ch6, –Ch4, –Ch5, +Ch2, –Ch3.

By analyzing the autocorrelation and cross-correlation properties of the SSFBGs, as shown in Figs. 5 and 6, respectively, we notice that all configurations present good autocorrelation and cross-correlation properties, with the configuration SSFBG3 presenting slightly worse autocorrelation, but still presenting a very distinctive in-phase peak. All configurations present a minimum power contrast ratio equal to 12.3 dB. The average power contrast ratio (defined as P/W=20log[Peak(Autocorrelation)/Average(Cross-correlation)]), is much larger and equal to 30.0 dB. P is the maximum value of the autocorrelation function of a signal and W is the average value of the cross-correlation function, using a logarithmic scale. The worst error probability has been found to be $\max\{P_e\}=5\times10^{-5}$.

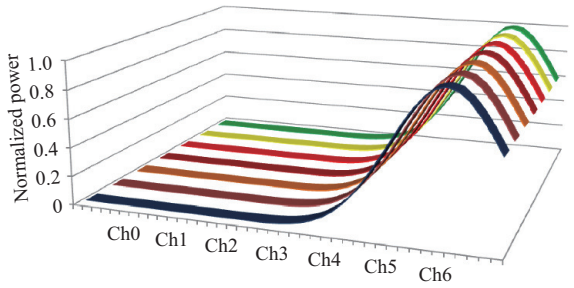

Fig. 4. Spectrum SSFBG3=+Ch6, +Ch6, +Ch6, –Ch6, –Ch6, +Ch6, –Ch6.

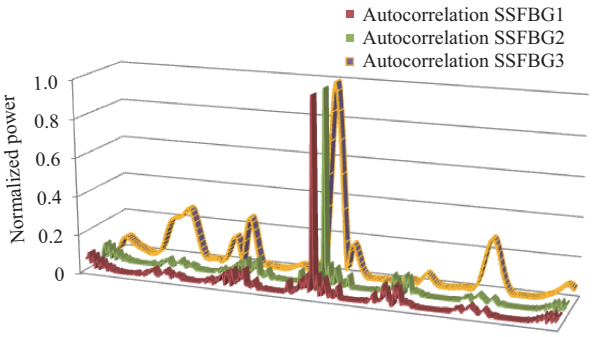

Fig. 5. Normalized autocorrelation, in time domain, with SSFBG1, SSFBG2, and SSFBG3.

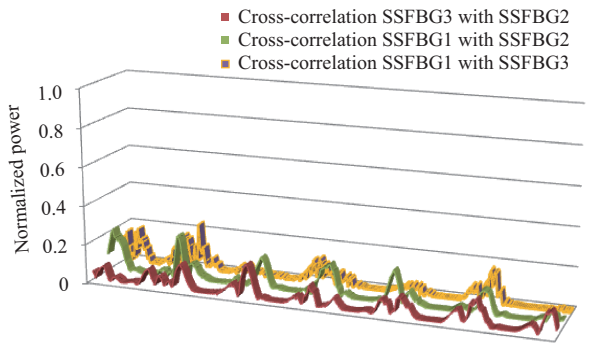

Fig. 6. Normalized cross-correlation, in time domain, with SSFBG1, SSFBG2, and SSFBG3.

4. Tunable SSFBG Error Probability

To simplify the study and analysis of the tunable SSFBG error probability, we chose to consider only bipolar codes (with two phases: 0 and π). The chip +1 is coded with a phase 0

and the chip –1 is coded with the phase π. The worst case to be considered is when the 7 chips are coded in the same wavelength channel. Then, the phase modulation is simply a binary phase shift keying (BPSK) modulation and the system to be analyzed is a time-spreading optical-code-division multiple-access passive-optical-network (TS-OCDMA-PON) system with coherent coding and decoding making use of bipolar codes. The error probability P_e may be used to find an upper bound for an OCDMA system. This P_e upper bound $\max\{P_e\}$ can be a function of the cross-correlation power contrast ratio $P/C = 20\log[C_k(0)/\max\{C_{k,i}\}]$ (in dB), where $C_{k,i}$ is the cross-correlation and C_k is the autocorrelation[2]. P is the value of the autocorrelation function, centered in zero, and C is the maximum value of the cross-correlation function, using a logarithmic scale. Some P/C upper bounds, for periodic correlations, have been found. One of them is the Welch bound[21] of K perfect sequences of length N: $P/C = 20\log\sqrt{(KN-1)/(K-1)}$. For the aperiodic correlation case, the upper bound is $P/C = 20\log\sqrt{(2KN-K-1)/(K-1)}$.

For a good communication system, the code set selected should have a high P/C value. For example, it has been suggested that the SSFBG should have power contrast ratios higher than 17 dB for 127-chips Gold codes[22].

In this study, we consider the upper bound of the error probability[2] that is a function of the power contrast ratio P/C:

$$\max\{P_e\} \approx 1-\phi\left[\left(\frac{N_0}{2E_b}+(K-1)\left(1-\frac{1}{N}\right)10^{-P/10C}\right)^{-1/2}\right]. \quad (13)$$

Fig. 7 shows a 3D representation of the upper bound (13), for $K=2$ users and the length is $N=7\times7$ chips. For example, the error probability upper bound is lower than 10^{-5} when the two ratios P/C and E_b/N_0 are at least equal to 12.3 dB. E_b is the bit energy and N_0 is the spectral density of additive white Gaussian noise (AWGN). ϕ is the normalized cumulative distribution function of Gauss (with zero-mean and unit-variance). This situation requires a bit error correction method to guarantee an error free transmission. However, we should remember that (13) gives us the worst case error probability. Frequently, the error probability average is utilized and, of course, this average will be much lower than the worst case (13).

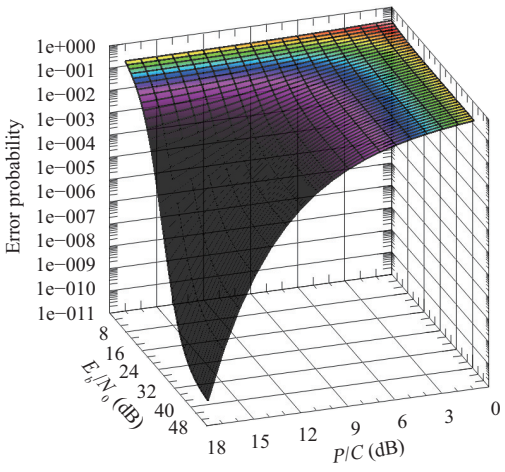

Fig. 7. 3D representation of the probability error upper bound with tunable SSFBG.

Finally, we should remember that the selection of the appropriate codes, the SSFBG ultraviolet light writing precision, and the precision of the optical communication synchronization (sampling operation) are important when we want to design a gigabit OCDMA-PON transmission system with a low bit error rate (BER) over more long distances.

5. Conclusions

In this paper, a new tunable SSFGB was developed by using stress-responsive colloidal crystals. A new SSFBG codec with nanoparticles has been simulated with a short maximal-length sequence. Using a mathematical model, we found that the novel tunable SSFBG is similar to a codec of perfect sequences. These sequences are, by definition, immune to multipath interferences.

Our proposed WDM-OCDMA system with coherent coding and decoding processes has been evaluated with an error probability based on the power contrast ratios of some code sets. The good results obtained allow the conclusion that the proposed tunable SSFBG, with colloidal crystals and perfect sequences, will be a simple solution for WDM-OCDMA communications, when the optical coding and decoding processes require the temperature stability and multiplexing capacity.

References

[1] H. Ding, Y. Cheng, H. Gu, Y. Zhao, B. Wang, and Z. Gu, "Tunable fiber Bragg grating based on responsive photonic crystals," *Nanoscale*, vol. 5, no. 23, pp. 11572:1-6, 2013.

[2] J. Pereira and H. A. Silva, "Error probability upper bound for perfect sequences implemented with super-structured fibre Bragg gratings," *IET Signal Processing*, vol. 8, no. 4, pp. 421-428, 2014.

[3] R. Matsumoto, T. Kodama, S. Shimizu, *et al.*, "40G-OCDMA-PON system with an asymmetric structure using a single multi-port and sampled SSFBG encoder/decoders," *Journal of Lightwave Technology*, vol. 32, no. 6, pp. 1132-1143, 2014.

[4] F. Idachaba, D. U. Ike, and O. Hope, "Future trends in fiber optics communication," *Lecture Notes in Engineering & Computer Science*, vol. 2211, no. 1, pp. 438-442, 2014.

[5] C. Lam, *Passive Optical Networks, Principles and Practice*, Elsevier, 2007.

[6] J. A. Salehi, A. M. Weiner, and J. P. Heritage, "Coherent ultrashort light pulse code division multiple access communication schemes," *Journal of Lightwave Technology*, vol. 8, no. 3, pp. 478-491, 1990.

[7] P. Prucnal, M. Santoro, and T. Fan, "Spread spectrum fiber-optic local area network using optical processing," *Journal of Lightwave Technology*, vol. 4, no. 5, pp. 547-554, 1986.

[8] M. A. Santoro and P. R. Prucnal, "Asynchronous fiber optic LAN using CDMA and optical correlation," *Proc. of the IEEE*, vol. 75, no. 9, pp. 1336-1338, 1987.

[9] M. Hadi and M. R. Pakravan, "Analysis and design of adaptive OCDMA passive optical networks," *Journal of Lightwave Technology*, vol. 35, no. 14, pp. 2853-2863, 2017.

[10] H. S. Abbas and M. A. Gregory, "The next generation of passive optical networks," *Journal of Network and Computer Applications*, vol. 67, no. C, pp. 53-74, 2016.

[11] S. Ahmed, M. S. Kh. Abuhelala, and I. Glesk, "Managing dispersion-affected OCDMA auto-correlation based on PS multiwavelength code carriers using SOA," *IEEE/OSA Journal of Optical Communications and Networking*, vol. 9, no. 8, pp. 93-698, 2017.

[12] H. Mrabet, I. Dayoub, and Rabah Attia, "Comparative study of 2D-OCDMA-WDM system performance in 40-Gb/s PON context," *IET Optoelectronics*, vol. 11, no. 4, pp. 141-147, 2017.

[13] S. Nlend, T. G. Swart, and B. Twala, "An access optimization approach for FFH-OCDMA system's fiber Bragg gratings encoder," in *Proc. of 2017 IEEE AFRICON*, 2017, pp. 348-353.

[14] K. Okamoto, "Recent progress of integrated optics planar lightwave circuits," *Optical and Quantum Electronics*, vol. 31, no. 2, pp. 107-129, 1999.

[15] Z. Jiang, D. Seo, S. Yang, *et al*., "Four-user 10-Gb/s spectrally phase-coded O-CDMA system operating at ~30 fJ/bit," *IEEE Photonics Technology Letters*, vol. 17, no. 3, pp. 705-707, 2005.

[16] X. J. M. Leijtens, B. Kuhlow, and M. K. Smi. Arrayed waveguide gratings. [Online]. Available: http://alexandria.tue.nl/openaccess/Metis203741.pdf

[17] T. Erdogan, "Fiber grating spectra," *Journal of Lightwave Technology*, vol. 15, no. 8, pp. 1277-1294, 1997.

[18] S. Blais. Superstructured fiber Bragg gratings and applications in microwave signal processing. (2014). [Online]. Available: https://www.ruor.uottawa.ca/bitstream/10393/30358/3/Blais_Sebastien_2014_thesis.pdf

[19] P. C. Teh, M. Ibsen, L. B. Fu, J. H. Lee, Z. Yusoff, and D. J. Richardson, "A 16-channel OCDMA system (4 OCDM ×4 WDM) based on 16-chip, 20 Gchip/s superstructure fiber Bragg gratings and DFB fiber laser transmitters," in *Proc. of Optical Fiber Communication Conf.*, 2002, pp. 600-601.

[20] J. Pereira, *Sequências Perfeitas Para Sistemas de Comunicação*, Saarbrücken: Novas Edições Acadêmicas, 2015.

[21] D. Sarwate and M. Pursley, "Crosscorrelation properties of pseudorandom and related sequences," *Proc. of the IEEE*, vol. 68, no. 5, pp. 593-619, 1980.

[22] X. Wang, K. Matsushima, A. Nishiki, N. Wada, and K. Kitayama, "High reflectivity super structured FBG for coherent optical code generation and recognition," *Optics Express*, vol. 12, no. 22, pp. 5457-5468, 2004.

João S. Pereira received the B.S., M.S., and Ph.D. degrees from University of Coimbra, Coimbra, Portugal in 1992, 2002, and 2013, respectively. Before 1987, he started the B.S. degree in higher mathematics at La Martinière Monplaisir, Lyon, France. After 1992, he worked for Ford Motor Company as a product engineer. Since 1997, he has been with the Polytechnic Institute of Leiria, Leiria, Portugal where, currently, he is an assistant professor in network engineering. Simultaneously, he is an optical communication researcher at Instituto de Telecomunicações, Lisboa, Portugal. He is also an IEEE Senior Member. His last book (2015) is related to Perfect Sequences for Communication Systems. His research interests include signal processing, wireless and optical communication systems, and more recently Internet of things (IoT) technologies.

Marco P. M. Ferreira received the B.S. degree in computer science from the Polytechnic Institute of Leiria in 2002. He is currently a Ph.D. student at Extremadura University, Badajoz, Spain. His research interests include metaheuristic algorithms and indoor positioning systems.

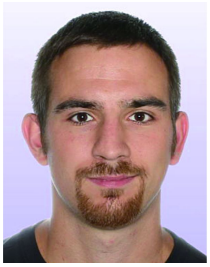

Marko Gasparovic received the B.S. degree in computer science from the Polytechnic Institute of Zagreb, Croatia in 2015. He is currently pursuing his M.S. degree in computer science with the Department of Mobile Computing, Polytechnic of Leiria, guided by Prof. J. S. Pereira. His current research as a part of master thesis work is based on indoor positioning system among others.